GEOPHYSICAL RESEARCH LETTERS
December2002; 29(23) : NIL_21-NIL_24
http://dx.doi.org/10.1029/2002GL015524

An edited version of this paper was published by AGU.

Sea surface state measured using GPS reflected signals

Antonio Rius[1], Josep M. Aparicio[1], Estel Cardellach[1], Manuel Martin-Neira[2], Bertrand Chapron[3*]

[1]Institut d'Estudis Espacials de Catalunya (IEEC/CSIC), Barcelona, Spain
[2]ESTEC, Noordwijk, The Netherlands
[3]IFREMER, Brest, France

*: Corresponding author : Bertrand.Chapron@ifremer.fr

Abstract: We discuss an airborne experiment aimed to establish the potential of the PARIS concept (PAssive Reflectometry and Interferometry System) to retrieve small features in the sea surface topography. The date and location were chosen to coincide with a TOPEX/POSEIDON (T/P) overflight. The signals of the Global Positioning System (GPS) reflected off the sea surface are tracked and compared to the directly received ones, to compute the relative delays. The features detected in the peak tracking are likely caused by topographic and sea roughness variations. While very promising, these results open the challenge to use additional information to appropriately separate both contributions.

Keywords: Sea surface topography, Inerferometry, Reflectrometry, Signal analysis

Introduction

In 1993 [*Martín-Neira,* 1993], the PARIS concept was conceived to use the coded signals transmitted from navigation satellites, such as the USA GPS constellation, to perform sea surface altimetry. To assess the precision and accuracy of this concept, experiments have been performed, and recently [*Lowe et al.,* 2002], an altimetric precision of 5 centimeters, during 150 seconds, with an aircraft flying at 3000 meters height was demonstrated. Hereafter, we discuss results obtained from data gathered over a coastal sea area, where the sea surface topography presents features at the 50 cm level over horizontal scales of 30 Km.

The data model

To obtain a concise formulation we assume a plane mean sea surface in the zone were the signal is reflected. We ignore the dry hydrostatic and ionospheric delays, which either could be modeled with sufficient accuracy, or are common, in the case of the aircraft, to both direct and reflected propagation paths.

Direct signals are received with a zenith-looking antenna, while reflected signals are gathered with a nadir-looking one. For each reflected link, the reflection will take place around a specular point. The observable we will consider, is the relative delay $\Delta\rho$ between arrival times of each signal through the reflected ρ_r or the direct ρ_d paths:

$$\Delta\rho = \rho_r - \rho_d \tag{1}$$

The geometric delay: With the assumptions made so far, the relative delay can be modeled for each satellite in terms of the height H of the receiver over a reference ellipsoid, the sea surface height N of the specular point over the ellipsoid, and the elevation angle e of the transmitter, as seen from the specular point:

$$\Delta\rho_{geo} = 2(H - N) \cdot sin(e) \tag{2}$$

The scatterometric delay: The reflecting surface is not smooth at the scale of the GPS L1 wavelength (19 cm), creating a superposition of many signals reflected from different areas of the glistening surface. These reflections around the specular point will reach the receiver with a range of positive delays with respect to the idealized smooth surface reflection case. Figure 1 is a sketch of this overall contribution in the altimetric model.

Figure 1

Figure 1

This scatterometric induced delay can be numerically computed from the radar equation [*Zavorotny and Voronovich, 2000*], as implemented in [*Cardellach,* 2002]. Following an analytical stochastic model for bistatic reflections [*Elfouhaily et al.,* 2002], a closed form can also be derived that allows an explicit parameterization of this scatterometric delay as:

$$\rho_{sca} = \Delta\rho_{geo} \cdot \kappa \cdot (1 + sin^{-2}(e)) \tag{3}$$

This simplified formulation has been obtained using isotropic Gaussian statistics for the sea surface, and does not include effects that are known to impact experimental data (in particular, the receiving antenna gain pattern). Hence, without loss of generality, we retain its functional dependence, reading κ as an *effective isotropic wave slope variance.*

The system delay: We must also consider errors induced by the data extraction system ρ_{sys}. One component is produced by the fact that our system uses three time scales for tagging the data: GPS time, and the two times used for sampling each of the direct and the reflected signals. All times were later synchronized, using the recorded GPS signal, to better than $1\mu s$. For normal Doppler rates of the order of 1 Hz/s, this desynchronization leads to effects of 0.2 mm over 1000 s. Therefore, only a bias is needed to describe this effect.

The noise delay: The noise in the differential observables is the superposition of the noise through the direct and the reflected path. The direct component is discussed in the literature [*Spilker, 1996*]. For the reflected signal, we consider a transmission through a fading multipath channel [*Proakis,* 2000] with an assumed coherence time of 10 msec. Each time slot of 10 msec produces estimates of the delays for the satellites on view. This simple "time diversity" method allows us to estimate a value of the delay each 0.1 sec, with a noise level of the order of 3 meter, as shown in Figure 4, compatible with those shown in [*Lowe et al.,* 2002].

In addition we should consider other sources of noise, like multipath in the aircraft, actual knowledge of the true height of the aircraft, receiving antenna pattern variations, shape of the sea surface and other mismodelling and instrumental effects. These effects could be minimized by avoiding aircraft maneuvers during the experiment.

The altimetric model

Taking all the above terms, the model for the GPS satellite s, writes:

$$\Delta\rho^s = \Delta\rho^s_{geo} + \rho^s_{sca} + \Delta\rho^s_{noise} \tag{4}$$

The geometric term $\Delta\rho^s_{geo}$ is the largest, but an a-priori approximation $\Delta\hat{\rho}^s_{geo} = 2\left[\hat{H} - \hat{N}\right] \cdot sin(e^s)$ can be obtained with an accuracy better than 1 meter. Subtracting it, leads to:

$$\begin{aligned} \delta\rho^s &\equiv \Delta\rho^s - \Delta\hat{\rho}^s_{geo} \\ &= -2\delta N^s \cdot sin(e^s) + \rho^s_{sca} + \Delta\rho^s_{noise} \end{aligned} \tag{5}$$

The height above the a-priori expected surface, δN^s, and the effective wave slope variance κ are thus the parameters to be estimated.

The experiment and the data acquisition system

The experiment was performed on September 25, 2001. An aircraft, equipped with GPS-reflection instruments and a GPS-aided Inertial Navigation System, over-flew a segment of the T/P pass number 187, at ∼1000 m altitude and ∼ 70 m/s speed. This area shows topographic gradients associated with bathymetric canyons (see Figure 2), perfectly detectable in the T/P altimetric profiles. The configuration of specular points around the aircraft nadir during the experiment is shown in Figure 3.

Figure 2 $\boxed{\text{Figure 2}}$

Figure 3 $\boxed{\text{Figure 3}}$

The system for gathering the direct and the reflected signals consists in two TurboRogue receivers, modified to output the IF signals, and two SONY-2000 high speed digital recorders. The two receiver-recorder sets were respectively connected to an up-looking right circular polarized antenna (RCP) (i.e. normal GPS operation) and to a down-looking left circular polarized one (LCP) installed in the airplane.

Redundant GPS receivers were deployed along the coast for an accurate retrieval of the aircraft trajectory. The navigation data were processed independently by the Institut Cartographic de Catalunya using their standard procedures, and by us using the US National Geodetic Survey KARS package [*Mader,* 1996]. The positioning results were consistent to the decimetric level.

Data processing

We have chosen a section of the complete data set, which was free of aircraft maneuvers, to minimize undesired effects due to the changing geometry.

The two L1 signals, down-converted and 1-bit sampled at 20.456 MHz, have been complex cross-correlated, in blocks of 20456 samples, against models of the signals corresponding to the satellites selected. The models are phasors, obtained from the available C/A codes, and an interpolation of the phase obtained each second from the TurboRogue connected to the RCP antenna.

The complex correlation function was integrated coherently up to 10 msec, and the correlation amplitude for each 10 msec interval has been computed using a least squares fitting procedure to extract the delay corresponding to the maximum. Using sets of ten consecutive peak delays, the median of the delay value is obtained. We further subtracted the geometric part based on the retrieved aircraft trajectory using a GPS kinematic navigation solution, and an a-priori mean sea surface height estimation [*Wang, 2001*].

Figure 4

Figure 4

The $\delta\rho^s$ quantities after removing a constant bias, obtained for four selected satellites are shown in Figure 4. These data show that a) the differential process has removed the signature of the 20 meters peak-to-peak changes in the aircraft height, b) the noise level is of the order of 3 m for 0.1s, c) mean variations are detected for all satellites and, d) for satellites PRN28 and PRN02 there is a linear trend, reflecting the mismodelling effects, which has been later removed for further processing.

Altimetry and scatterometry

From the altimetric model, the residual embedded signals are related to the scatterometric delay and the differential height δN^s. Using peak tracking estimates, and given the small variation in elevation for each satellite during the experiment, both contributions cannot be extracted independently.

Figure 5 shows the solution obtained neglecting ρ^s_{sca}, i.e. the observable residuals would be exclusively related to the sea surface topography (*topographic interpretation*). In Figure 6, we assume as perfectly known the geometry of the problem, and only the variation of κ^s in Equation (3) is inferred from ρ^s_{sca} (*scatterometric interpretation*). The a-priori geometry is taken from the mean sea surface profile, which shows a maximum variation of 30 cm [*Wang, 2001*]. In both cases we applied a horizontal filtering of 15 km.

Figure 5 Figure 5

Figure 6 Figure 6

The sea level profile obtained under the topographic interpretation, compared to the T/P estimate, shows differences larger than one meter. This might result from the use of an adjustment of the altimetric solution at both ends of the analyzed track. Consequently, true differences might be smaller than reported. On the other hand, the variations $\Delta\kappa^s$ of the estimated κ^s and the variations $\Delta\sigma^0_{dB}$ of the T/P radar cross section are shown to both follow an apparent increase in local sea surface roughness. This suggests that the information contained in the effective κ^s can efficiently be related to the sea surface roughness changes over this local region.

Conclusions

The processing of the airborne gathered GPS reflected data yields altimetric observables with a precision level of the order of 3m for 0.1 sec, a value compatible with the retrieval of the sea surface topographic signature of 50 cm in 30 km. This study, solely considering a peak tracking measurement, highlighted the expected impact of sea surface roughness. Following a reduced formulation of this scatterometric component, the effective wave slope variance κ^s tracked local T/P radar cross section measurements. In principle, the observed features must be interpreted as combined altimetric and scatterometric effects. Future research should then be performed to take full advantage of complete GPS reflected waveform analysis, to further complement peak tracking measurements and to better assess the accuracy and precision of the concept.

Acknowledgments

This experiment has been funded by the Contract ESA ESTEC 14285/00/NL/PB. IEEC has received partial support from grants MCYT REN2001/2135 and DURSI PIRA2001/00244. We would like to acknowledge all the participants and institutions that contributed to the experimental campaign: María Belmonte (ESTEC/ESA) and Giulio Ruffini (Starlab-BCN) in the design phase; the whole IEEC GOT team, Starlab-BCN team, Centre de Supercomputació de Catalunya, Institut Cartogràfic de Catalunya (ICC) flights group and Agustí Julià (ICM) for their participation in the campaign; and Pablo Colmenarejo (GMV) and Julià Talaya (ICC) for the aircraft kinematic processing. A. R. would like to acknowledge S.J.Lowe (JPL) for discussions on data processing. We also wish to thank the anonymous reviewers for their useful comments.

References

Cardellach, E. Sea surface determination using GNSS reflected signals Ph.D. thesis, 199 pp., Universitat Politècnica de Catalunya and Institute for Space Studies of Catalonia (IEEC), March 2002.

Elfouhaily, T., D. R. Thompson and L. Linstrom, Delay-Doppler Analysis of Bistatically Reflected Signals From the Ocean Surface: Theory and Application, *IEEE Transactions on Geoscience and Remote Sensing*, *40 # 3,* 560–573, 2002.

Lowe, S. T., C. Zuffada, Y. Chao, P. Kroger, J. L. LaBrecque, L. E. Young, 5-cm-Precision Aircraft Ocean Altimetry Using GPS Reflections, *Geophys. Res. Lett.,* 10.1029/2002GL014759, 2002.

Mader, G.L., Kinematic and rapid static (KARS) GPS positioning: techniques and recent results, Proceedings IAG Symposium No. 115, 'GPS trends in terrestrial, airborne and spaceborne applications', XXI General Assembly of IUGG, Boulder, CO, July 2-14, 1995, G. Beutler et.al. (Eds.), Springer Verlag, pp. 170-174, 1996.

Martín-Neira, M., A passive reflectometry and interferometry system (PARIS): application to ocean altimetry *ESA Journal*, *17,* 331-355, 1993.

Proakis, J. G., Digital Communications, 4th Ed., McGraw Hill, 2000.

Spilker, J. J., Signal Structure and theoretical performance, in *Global Positioning System: Theory and Applications, Ed. B. Parkinson and J. J. Spilker, American Institute of Aeronautics and Astronautics. Inc*, vol. 1, 57-119, 1996.

Wang, Y.M., GSFC00 mean sea surface, gravity anomaly and vertical gravity gradient from satellite altimeter data, *J. Geophys. Res.,* , *106*, 31167-31174, 2001.

Zavorotny, V.U., and A. Voronovich, Scattering of GPS signals from the ocean with wind remote sensing application, *IEEE Transactions on Geoscience and Remote Sensing*, *38, No.2,* 951-964, 2000.

A. Rius, J. M. Aparicio and E. Cardellach, Institut d'Estudis Espacials de Catalunya (IEEC/CSIC), Gran Capità, 2, #204, 08034 Barcelona, Spain. (e-mail: rius@ieec.fcr.es, aparicio@ieec.fcr.es, estel@ieec.fcr.es)

M. Martín-Neira, European Space Research and Technology Centre (ESTEC), European Space Agency (ESA), Noordwijk, The Netherlands. (e-mail: Manuel.Martin-Neira@esa.int)

B. Chapron, IFREMER Centre de Brest, BP 70, 29280 Plouzané France. (e-mail: bertrand.chapron@ifremer.fr)

Received ____________________

To appear in the *Geophysical Research Letters*, 2002.

Figure 1. Sketch of the geometric and scatterometric contributions to the observables. The roughness of the surface increases the peak to peak delay beyond the geometric amount.

Figure 2. Map of the experiment. The flight path along the T/P track. The circles indicate the resolution of the T/P Radar Altimeter. The reference stations are marked, and the processed segment is highlighted.

Figure 3. Specular point position relative to the aircraft nadir. The circles represent the relative gain of the nadir-looking antenna. The arrow indicates the direction of the flight.

Figure 4. Raw observables: $\delta\rho^s$ for each selected satellite, in meters vs. time in *seconds of the day*. There is a point each 0.1 s. Solid line: scatterometric extra delay as computed with the implementation of the radar equation assuming the sea surface roughness given by the Ku band of the T/P radar altimeter.

Figure 5. Topographic interpretation: Variations of the sea surface height δN^s obtained for each satellite vs. latitude.The long-term averaged topographic profile according to [*Wang, 2001*] and the measured in this pass by T/P are also shown.

Figure 6. Scatterometric interpretation: variations of the effective covariance κ^s of the sea slopes for each satellite vs.latitude (left scale).The variation of the T/P σ^0_{Ku} is overplotted with inverted triangles (the empty one is less reliable, right scale).

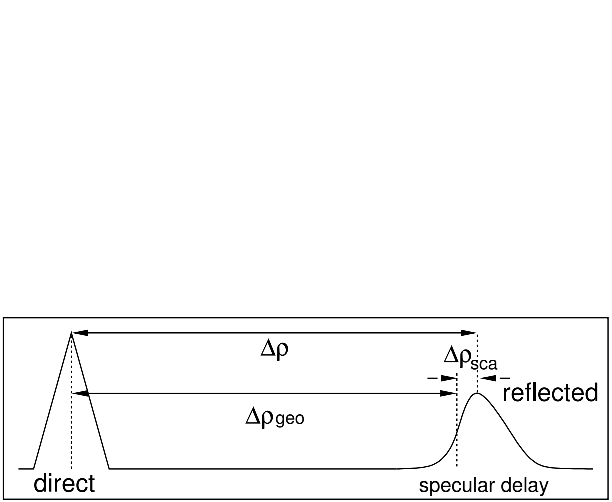

Δρ
Δρsca
reflected
Δρgeo
direct
specular delay

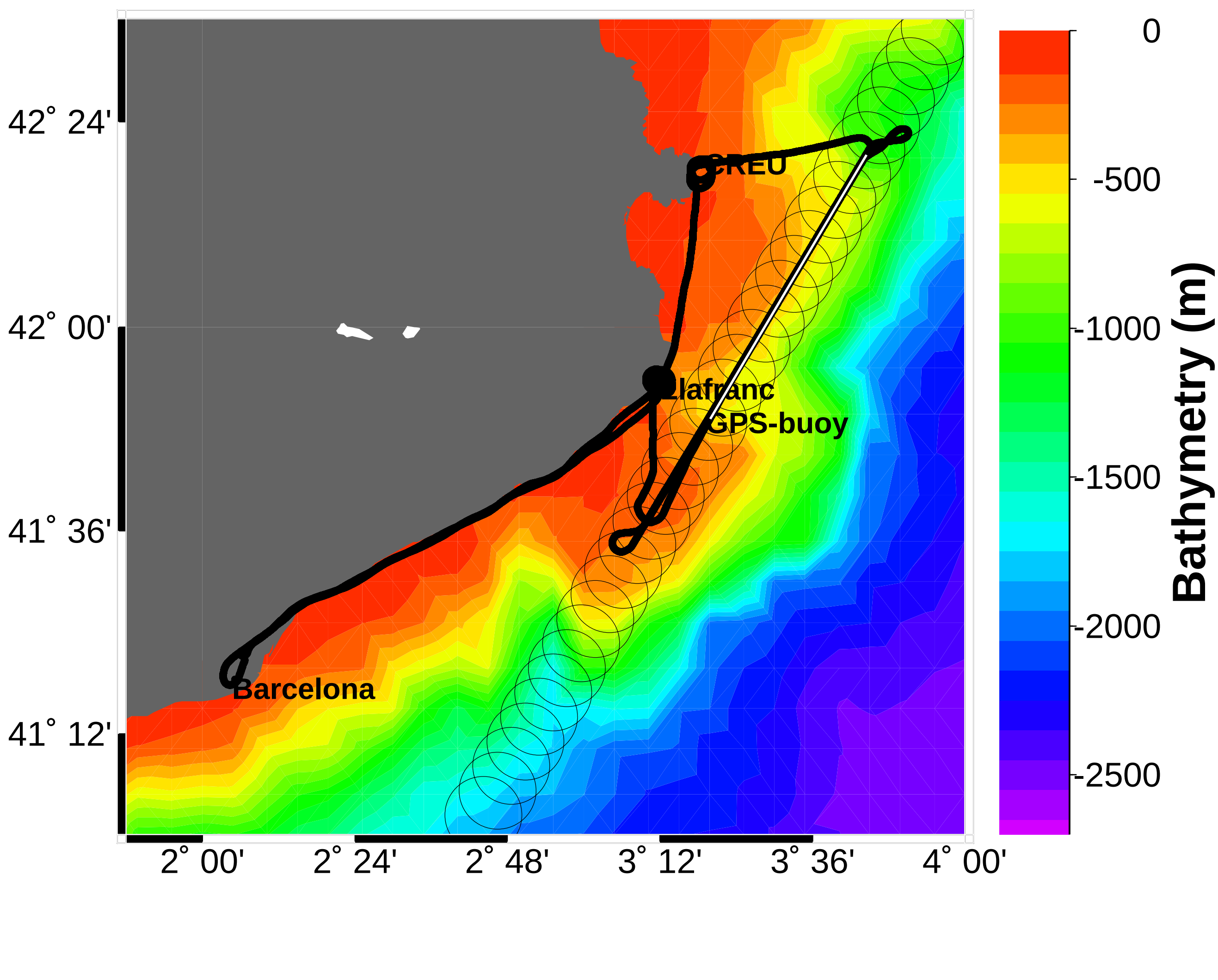

CREU
Llafranc
GPS-buoy
Barcelona
42° 24'
42° 00'
41° 36'
41° 12'
2° 00'
2° 24'
2° 48'
3° 12'
3° 36'
4° 00'
0
-500
-1000
-1500
-2000
-2500
Bathymetry (m)

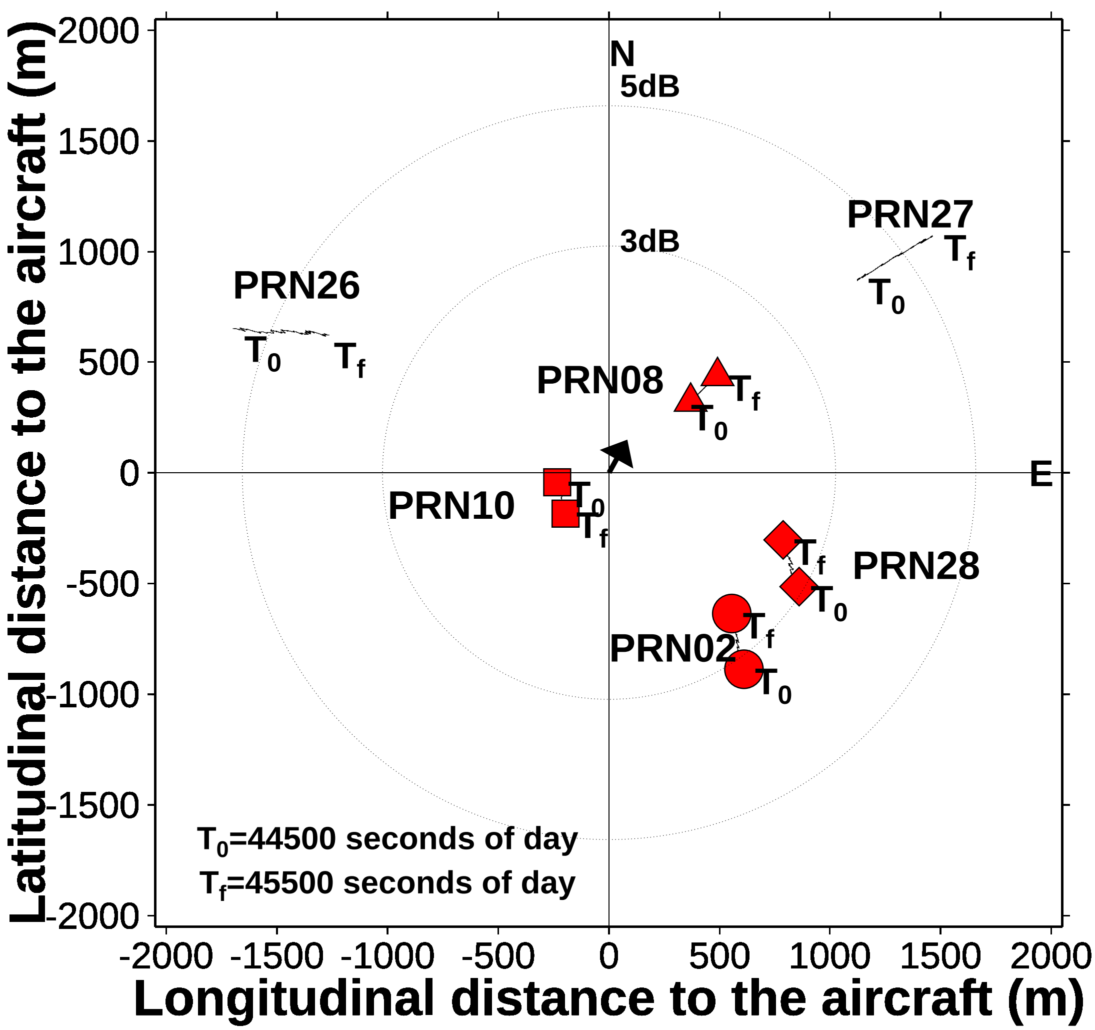

N
5dB
3dB
E
PRN27
PRN26
PRN08
PRN10
PRN28
PRN02
T0
Tf
T0=44500 seconds of day
Tf=45500 seconds of day
2000
1500
1000
500
0
-500
-1000
-1500
-2000
Latitudinal distance to the aircraft (m)
Longitudinal distance to the aircraft (m)

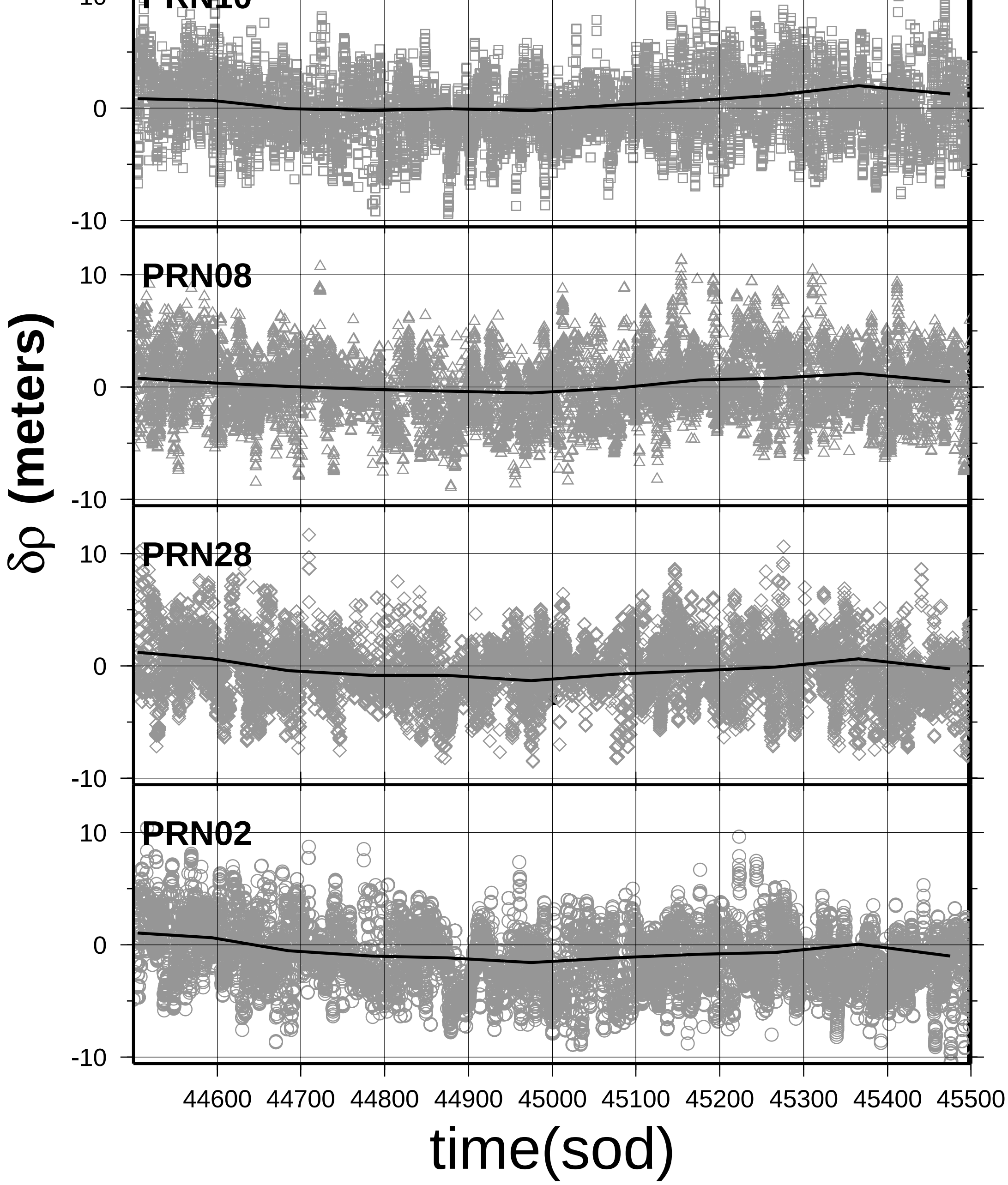
PRN10
PRN08
PRN28
PRN02
δρ (meters)
10
0
-10
44600
44700
44800
44900
45000
45100
45200
45300
45400
45500
time(sod)

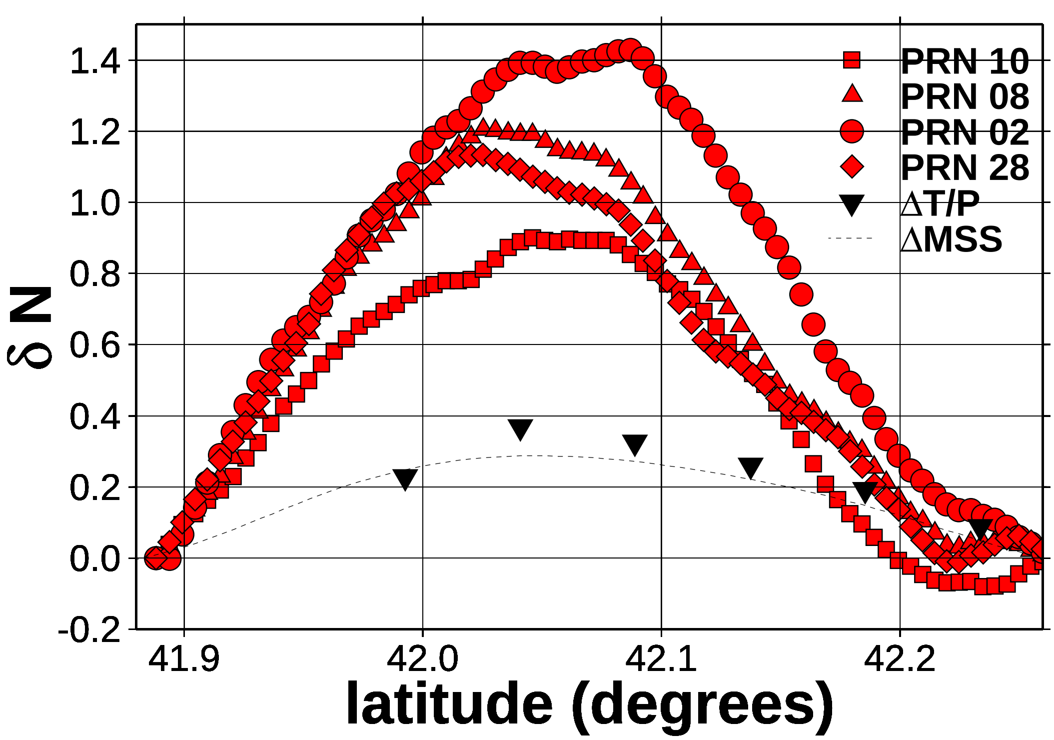

PRN 10
PRN 08
PRN 02
PRN 28
ΔT/P
ΔMSS
δ N
latitude (degrees)
1.4
1.2
1.0
0.8
0.6
0.4
0.2
0.0
-0.2
41.9
42.0
42.1
42.2

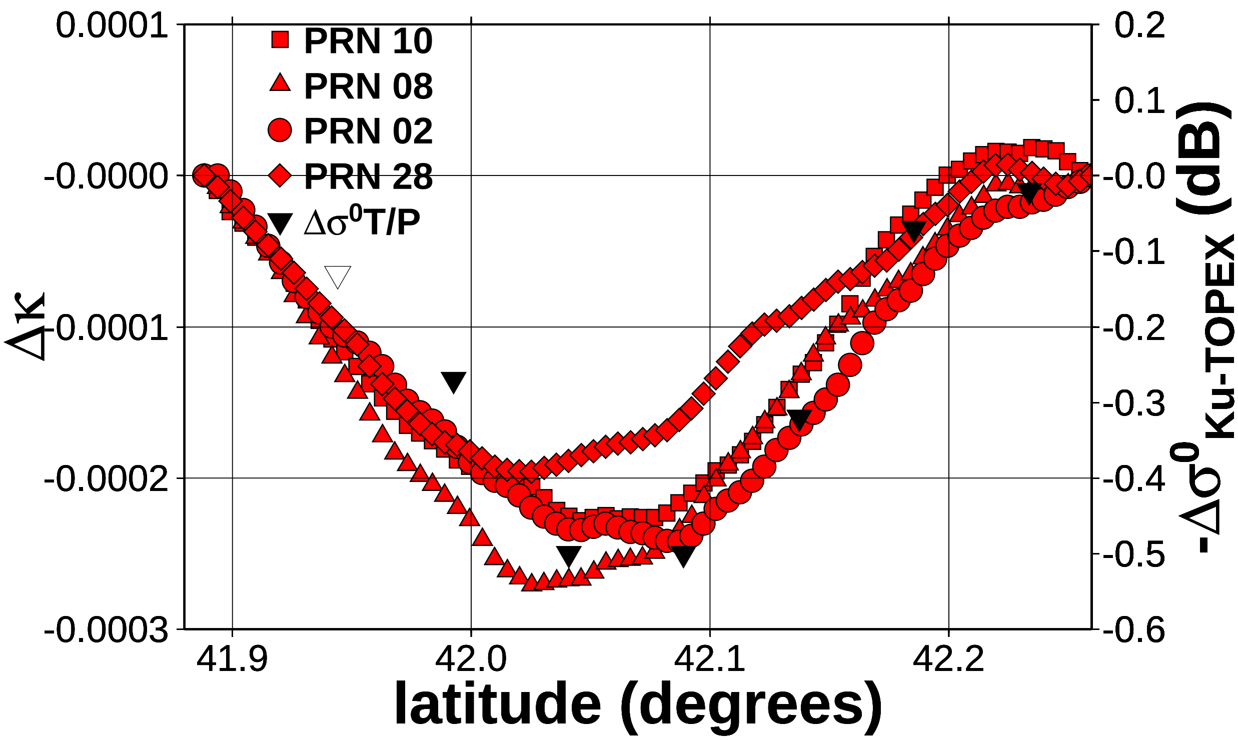

PRN 10
PRN 08
PRN 02
PRN 28
Δσ⁰T/P
Δκ
0.0001
-0.0000
-0.0001
-0.0002
-0.0003
0.2
0.1
-0.0
-0.1
-0.2
-0.3
-0.4
-0.5
-0.6
41.9
42.0
42.1
42.2
latitude (degrees)
-Δσ⁰Ku-TOPEX (dB)